



Vancomycin Is Protective in a Neonatal Mouse Model of *Staphylococcus epidermidis*-Potentiated Hypoxic-Ischemic Brain Injury

 Jacqueline C. Y. Lai,^{a,b,c}
 Pernilla Svedin,^a
 C. Joakim Ek,^a
 Amin Mottahedin,^a
 Xiaoyang Wang,^{a,e}
 Ofer Levy,^{b,c,d}
 Andrew Currie,^{f,g}
 Tobias Strunk,^{f,h}
 Carina Mallard^{a,e}

^aCenter for Perinatal Medicine and Health, Department of Physiology, Institute of Neuroscience and Physiology, Sahlgrenska Academy, University of Gothenburg, Gothenburg, Sweden

^bPrecision Vaccines Program, Division of Infectious Diseases, Boston Children's Hospital, Boston, Massachusetts, USA

^cHarvard Medical School, Harvard University, Boston, Massachusetts, USA

^dBroad Institute of Harvard and MIT, Cambridge, Massachusetts, USA

^eHenan Key Laboratory of Child Brain Injury, Third Affiliated Hospital of Zhengzhou University, Zhengzhou, China

^fCentre for Neonatal Research and Education, University of Western Australia, Perth, Western Australia, Australia

^gMedical, Molecular and Forensic Sciences, Murdoch University, Perth, Western Australia, Australia

^hNeonatal Directorate, King Edward Memorial Hospital for Women, Subiaco, Western Australia, Australia

ABSTRACT Infection is correlated with increased risk of neurodevelopmental sequelae in preterm infants. In modeling neonatal brain injury, Toll-like receptor agonists have often been used to mimic infections and induce inflammation. Using the most common cause of bacteremia in preterm infants, *Staphylococcus epidermidis*, we present a more clinically relevant neonatal mouse model that addresses the combined effects of bacterial infection together with subsequent hypoxic-ischemic brain insult. Currently, there is no neuroprotective treatment for the preterm population. Hence, we tested the neuroprotective effects of vancomycin with and without adjunct therapy using the anti-inflammatory agent pentoxifylline. We characterized the effects of *S. epidermidis* infection on the inflammatory response in the periphery and the brain, as well as the physiological changes in the central nervous system that might affect neurodevelopmental outcomes. Intraperitoneal injection of postnatal day 4 mice with a live clinical isolate of *S. epidermidis* led to bacteremia and induction of proinflammatory cytokines in the blood, as well as transient elevations of neutrophil and monocyte chemotactic cytokines and caspase 3 activity in the brain. When hypoxia-ischemia was induced postinfection, more severe brain damage was observed in infected animals than in saline-injected controls. This infection-induced inflammation and potentiated brain injury was inoculum dose dependent and was alleviated by the antibiotic vancomycin. Pentoxifylline did not provide any additional neuroprotective effect. Thus, we show for the first time that live *S. epidermidis* potentiates hypoxic-ischemic preterm brain injury and that peripheral inhibition of inflammation with antibiotics, such as vancomycin, reduces the extent of brain injury.

KEYWORDS *Staphylococcus epidermidis*, bacterial infection, sepsis, hypoxia-ischemia, neonatal mice, vancomycin, pentoxifylline, brain injury, neuroprotection, preterm

Preterm birth poses a major challenge for perinatal medicine, contributing to over 40% of perinatal mortality in infants born at 23 weeks of gestation in developed countries (1). Compared to term infants, infants that survive preterm birth are more likely to suffer respiratory, visual, and hearing impairment and have neurodevelopmental problems. Currently, there is a lack of neuroprotective treatments for the preterm population. While maternal infection increases the risk of preterm birth, postnatal

Citation Lai JCY, Svedin P, Ek CJ, Mottahedin A, Wang X, Levy O, Currie A, Strunk T, Mallard C. 2020. Vancomycin is protective in a neonatal mouse model of *Staphylococcus epidermidis*-potentiated hypoxic-ischemic brain injury. *Antimicrob Agents Chemother* 64:e02003-19. <https://doi.org/10.1128/AAC.02003-19>.

Copyright © 2020 American Society for Microbiology. All Rights Reserved.

Address correspondence to Jacqueline C. Y. Lai, jacqueline.lai@neuro.gu.se, or Carina Mallard, carina.mallard@neuro.gu.se.

Received 4 October 2019

Returned for modification 20 October 2019

Accepted 6 December 2019

Accepted manuscript posted online 9 December 2019

Published 21 February 2020

infections and their associated inflammation are also independently correlated with brain injury affecting neurodevelopmental outcomes (2). Acute asphyxia followed by developmental arrest of brain processes leading to hypoxic-ischemic encephalopathy (HIE) is more common in preterm than in term infants (1). Factors leading to HIE in preterm infants are complex, with multifactorial etiology involving concurrent processes, such as inflammation, hypoxia-ischemia (HI) and excitotoxicity (3). Supporting this, a significant number of animal studies have shown that the combination of innate immune activation, via addition of a pattern recognition receptor agonist, and cerebral HI increases the vulnerability of the developing brain, leading to brain injury (2).

Almost one-third of preterm infants admitted into neonatal intensive-care units experience at least one episode of confirmed culture-positive sepsis, predominately with Gram-positive coagulase-negative staphylococci (4). *Staphylococcus epidermidis* is the most common cause of nosocomial or late-onset sepsis (LOS) in preterm infants. Although the overall mortality of *S. epidermidis* LOS is low, the rate can be as high as 10% in very-low-birth-weight infants (5). In addition, the long-term health consequences for surviving neonates and associated health care costs are significant (6). *S. epidermidis* dominates the skin flora, and LOS is partly related to the microorganism adhering as biofilms to intravascular catheters, posing a threat to infants once the bacteria dislodge and enter the bloodstream (7). Due to high rates of resistance of coagulase-negative staphylococci to methicillin, vancomycin has become the choice for treatment of neonatal sepsis. However, since biofilms are highly resistant to antibiotics, a search for adjunct therapies to boost immune defenses in newborns is needed (8). In particular, the immunomodulating drug pentoxifylline (PTX) has been investigated as a potential candidate (9, 10). PTX is effective in decreasing mortality in septic adult and neonatal patients (11), increasing cerebral blood flow (CBF) in patients with cerebrovascular diseases (12) and providing neuroprotection in experimental models of neonatal HI (13–15), rendering it a candidate adjunctive therapy (i.e., along with antibiotics) for neonates experiencing sepsis and HIE.

Advances in developing treatments for sepsis and HIE depend in part on predictive animal models. Previously, Toll-like receptor (TLR) agonists have been used to mimic infection in neonatal mice, but the use of these pure agonists does not fully recapitulate the pathophysiology of infection with live microbes (16–18). Here, we introduce for the first time an animal model of preterm HI brain injury where HI is combined with systemic live-bacterial infection using a clinical isolate of *S. epidermidis* (the SE-HI model) and postnatal day 4 (PND4) mice, where the brain is developmentally equivalent to that of preterm infants (19, 20).

RESULTS

Intraperitoneal injection of *S. epidermidis* leads to self-clearing bacteremia and systemic cytokine response. To characterize the effects of infection and inflammation on the developing brain, neonatal mice were injected intraperitoneally (i.p.) with two sublethal inocula of *S. epidermidis*. Mice injected with the lower inoculum of 1×10^7 CFU ($n = 6$) did not produce significant levels of interleukin 6 (IL-6) or CCL2 in the serum (see Fig. S1 in the supplemental material), nor did this dose affect neuropathology (see Fig. S2A in the supplemental material), and subsequent experiments were thus performed with the higher *S. epidermidis* inoculum of 3.5×10^7 CFU per animal. In the absence of any intervention, the survival rate of the animals past 24 h after the injection of 3.5×10^7 CFU was 94% (203 out of a total of 216 mice used in this study).

Intraperitoneal injection can lead to entry of the bacteria into the bloodstream via lymphatic drainage prior to systemic dissemination throughout the animal (21, 22). Indeed, bacteremia was observed in 10 out of 12 mice within 2 h of intraperitoneal administration of *S. epidermidis* into PND4 animals, with 8 of the 10 animals having blood CFU counts above the detection threshold of 2,000 CFU/ml of blood (Fig. 1A). Successful injection of bacteria into each animal was confirmed by the presence of *S. epidermidis* in the spleen (Fig. 1A). The concentration of bacteria detected in the blood was highest at 2 h postinjection. By 48 h, clearance of the bacteria from the blood to

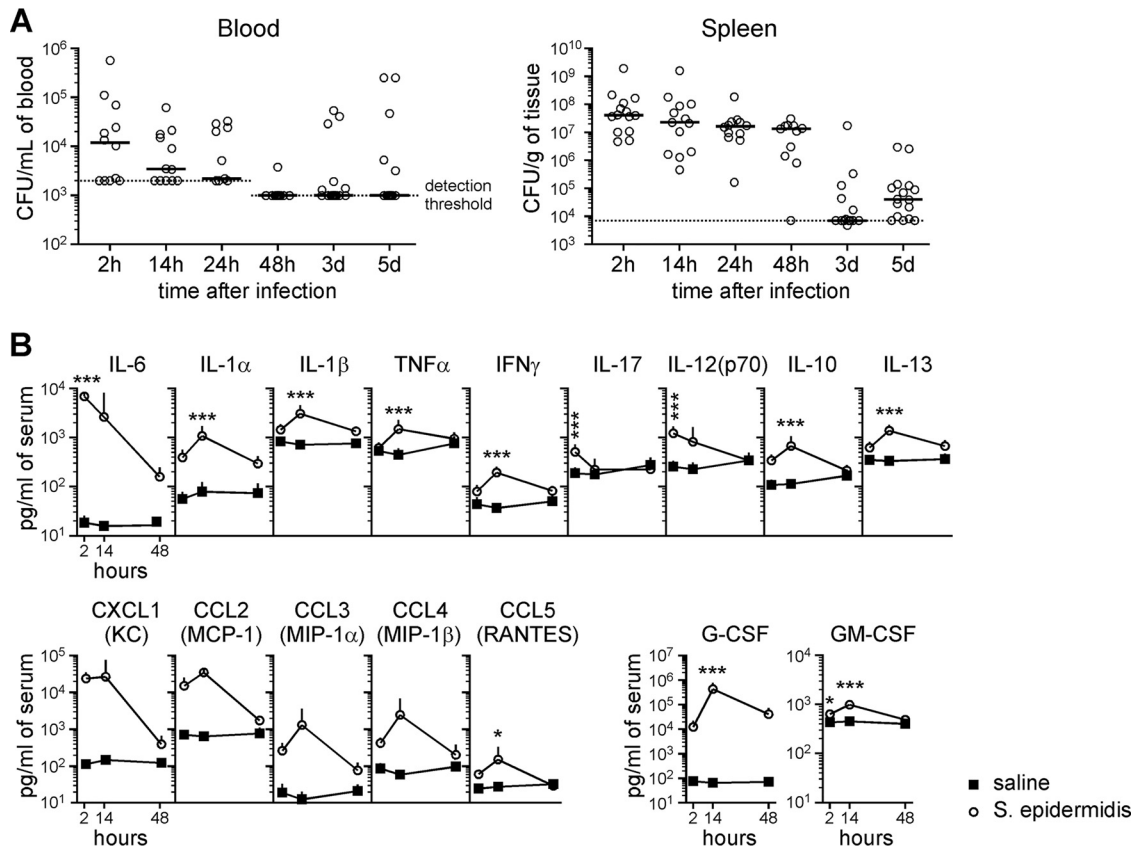


FIG 1 Intraperitoneal injection of *S. epidermidis* results in bacteremia and organ infection in PND4 mice. Mice i.p. injected with 3.5×10^7 CFU *S. epidermidis* at PND4 were sacrificed for blood CFU enumeration and cytokine analysis at various times after infection. (A) Bacterial-cell counts in the peripheral blood and spleen. The solid lines depict medians. The dotted lines represent detection thresholds. The data shown are pooled from at least 3 independent experiments ($n = 10$ to 17 mice per time point). (B) Multiplex cytometric bead array analysis of sera 2 to 48 h after i.p. injection of saline or *S. epidermidis*. The data are expressed as means plus SD of 8 infected mice and 6 saline controls from at least three litters. Statistical analysis employed two-way ANOVA with the Bonferroni *post hoc* test (*, $P < 0.05$; ***, $P < 0.001$).

below the detection threshold of 1,000 CFU/ml of blood was observed in a majority (10 out of 11) of animals. No CFU were observed in the cerebrospinal fluid (CSF) sampled from infected mice 14 h postinfection ($n = 10$) (data not shown).

To understand the immune response elicited by the bacterial infection, sera from peripheral blood samples were analyzed for a panel of inflammatory cytokines (Fig. 1B; see Table S1 in the supplemental material). A wide range of proinflammatory and anti-inflammatory cytokines were produced, with the response of IL-6 and IL-1 α the most significant. Chemotactic cytokines, including the neutrophil chemoattractant CXCL1 (KC) and the monocyte/macrophage chemoattractant CCL2 (MCP-1) were produced, and the granulocyte colony-stimulating factor (G-CSF), which stimulates the production of granulocytes from the bone marrow and their mobilization into the bloodstream, was upregulated. With the exceptions of IL-6 and CXCL1, for which the highest cytokine concentration was detected as early as 2 h postinfection, most other cytokines showed the highest levels at 14 h, and almost all the cytokines returned to homeostatic levels by 48 h postinfection.

Since pyrogenic cytokines were produced by the infected mice, we monitored the rectal temperature of treated animals over time and found no significant fluctuation in body temperature between the saline- and *S. epidermidis*-injected groups (Fig. 2A). The body weights of mice in the infected group (2.7 ± 0.5 g; $n = 22$) were significantly reduced compared to the control group (3.4 ± 0.4 g; $n = 22$; $P < 0.001$) at 24 h postinfection. Normalizing the body weight of each animal to its weight prior to injection, body weight gain was impaired in infected animals compared to saline

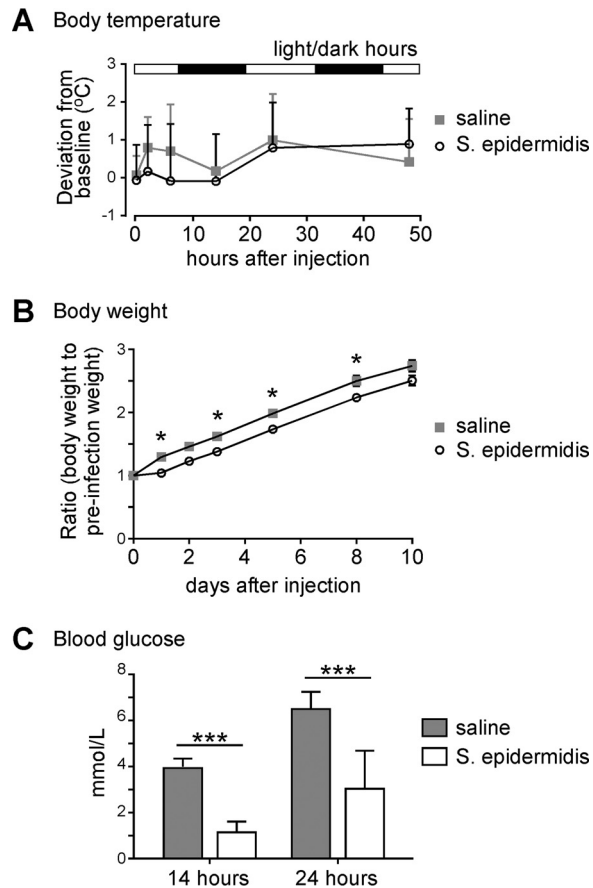


FIG 2 *S. epidermidis* infection impairs body weight gain and decreases blood glucose. Mice injected with saline or *S. epidermidis* at PND4 were monitored for body temperature, body weight, and blood glucose over time. (A) Rectal temperature deviation from the mean temperature of the litter prior to treatment. Means plus SD are plotted. The data were pooled from 3 independent experiments (saline, $n = 11$; *S. epidermidis*, $n = 13$). Statistical analysis employing two-way repeated-measures ANOVA showed no significant difference between the two treatment groups. (B) Weight gain. The data were pooled from 5 independent experiments. Means for the litter \pm standard errors of the mean (SEM) are plotted ($n = 7$ litters). Statistical analysis employed two-way repeated-measures ANOVA with the Bonferroni *post hoc* test (*, $P < 0.05$). (C) Blood plasma glucose measurements taken at 14 or 24 h postinfection. Means plus SD are plotted ($n = 6$ to 9 mice per group). Statistical analysis employed two-way ANOVA with the Bonferroni *post hoc* test (***, $P < 0.001$).

controls (Fig. 2B), with a lag in weight gain that continued until at least 8 days postinfection. In addition, *S. epidermidis*-infected animals demonstrated significant decreases in blood glucose levels compared to saline controls at 14 and 24 h after injection (Fig. 2C).

Intraperitoneal injection of *S. epidermidis* does not affect brain development.

To determine if *S. epidermidis* infection alone at this age had an effect on brain development, we examined the white and gray matter volume in animals that were intraperitoneally injected with *S. epidermidis* at PND4. There was no difference in the brain-to-body-weight ratios between saline- and *S. epidermidis*-injected animals 10 days postinfection (at PND14). No difference in cerebral gray matter volume or regional white matter was observed (Fig. 3).

Infection with *S. epidermidis* potentiates HI brain injury. Inflammation, including TLR agonist-induced responses, can potentiate HI brain injury (16–18, 23). To more accurately model clinical disease in which a live microbial pathogen induces the inflammatory response, we combined *S. epidermidis* infection with an established model of HI. Mice were first injected with 3.5×10^7 CFU of *S. epidermidis*, and HI was induced 14 h later, a time when peripheral inflammatory cytokine levels are high. In

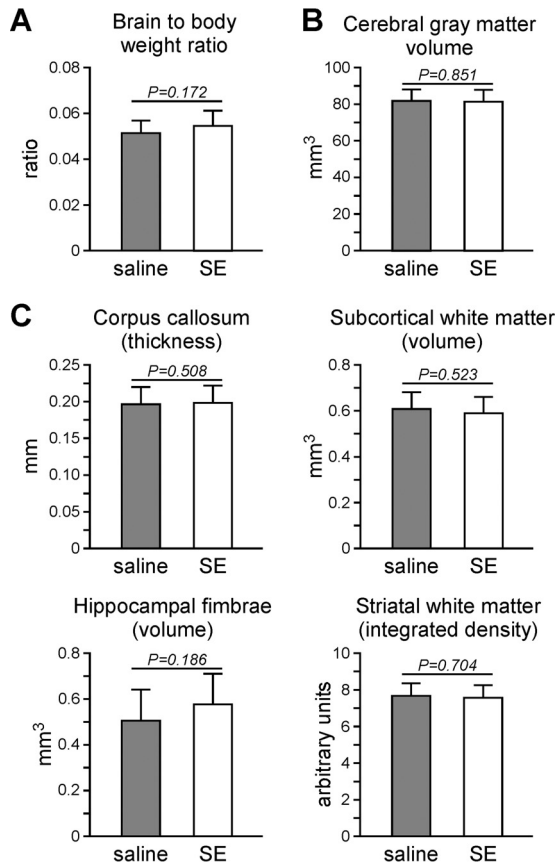


FIG 3 *S. epidermidis* infection alone did not affect the gross measurements of the brain 10 days postinfection. Mice injected with saline or *S. epidermidis* (SE) at PND4 were sacrificed at PND14 for analysis of the brain. (A) Means plus SD of the brain-to-body weight ratio ($n = 15$ or 16 mice per group from 5 litters). (B and C) Brain sections were stained for microtubule-associated protein 2 (B) or myelin basic protein (C) for gray and white matter quantification, respectively. Means plus SD of cerebral gray matter volume, regional white matter thickness or volume, and average integrated density across the striatum are presented. The data were pooled from two independent experiments with 13 mice per group. Statistical analysis employing Student's *t* test showed no statistical significance between saline- and *S. epidermidis*-treated animals.

animals experiencing HI alone ($n = 23$), the gray matter tissue loss was mostly localized to the hippocampus and, to a lesser extent, the striatum. However, when HI was combined with *S. epidermidis* infection (SE-HI; $n = 23$), increased injury/tissue loss was observed in all brain regions measured: the cortex (5.0 ± 5.1 versus 19.6 ± 21.0 [mean \pm standard deviation {SD}]; $P < 0.01$), hippocampus (34.7 ± 33.4 versus 72.4 ± 26.6 ; $P < 0.001$), and striatum (13.4 ± 14.6 versus 45.1 ± 26.7 ; $P < 0.0001$) compared to saline-injected mice experiencing HI (Fig. 4A). There was no significant difference in gray matter loss between males and females (see Fig. S2B). Analysis of white matter tissue loss by tissue volume or integrated density revealed that *S. epidermidis* significantly exacerbated HI white matter injury in the hippocampal fimbria and the striatum (Fig. 4B).

Vancomycin reduces peripheral inflammation and provides neuroprotection in *S. epidermidis*-potentiated HI brain injury. To test the hypothesis that infection/inflammation contributes to *S. epidermidis*-mediated potentiation of brain injury, we treated animals with vancomycin in the presence or absence of PTX. In *S. epidermidis*-infected animals, administration of vancomycin at the time of infection ($n = 11$) effectively decreased the number of viable bacteria detected in the spleen at 14 h postinfection (Fig. 5A) compared to saline-treated mice ($n = 9$). Caspase 3 activity and inflammatory cytokine levels in the periphery and the brain were also significantly reduced (Fig. 5B and C). Using PTX as an adjunct therapy to vancomycin did not

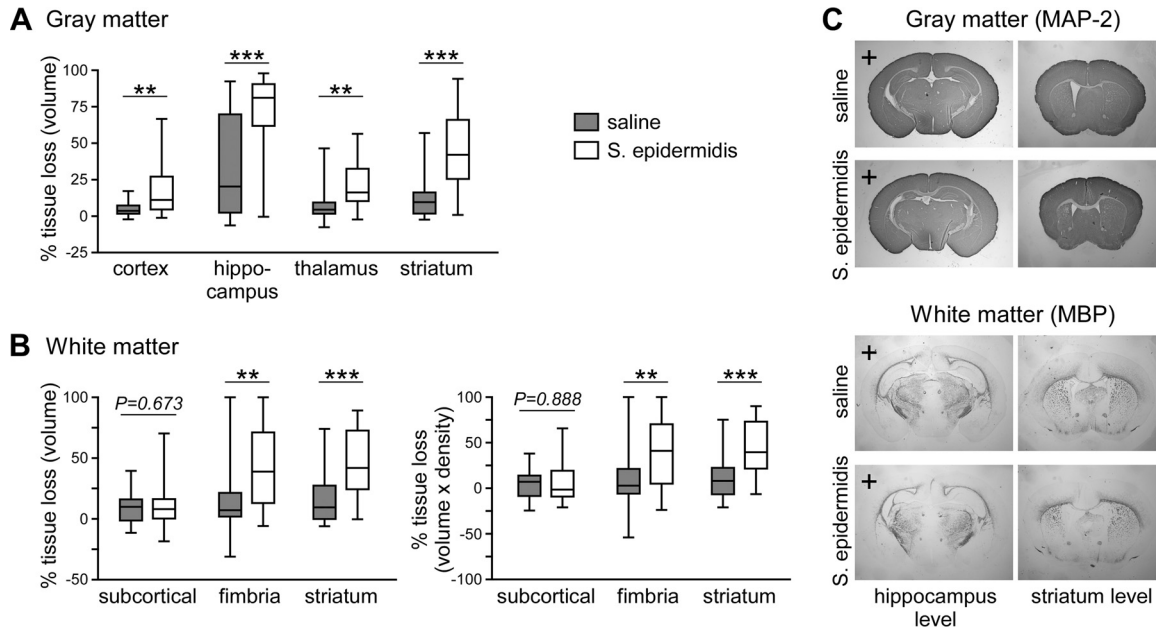


FIG 4 *S. epidermidis* infection 14 h prior to hypoxia-ischemia-enhanced brain injury. Hypoxia-ischemia was induced 14 h after injection of saline or *S. epidermidis* into PND4 mice ($n = 23$ per group). Brains were harvested 9 days later (on PND14), stained for microtubule-associated protein 2 (MAP-2) or myelin basic protein (MBP), and analyzed for tissue loss in the ipsilateral hemisphere. (A) Percentages of gray matter tissue loss in individual cerebral regions. (B) White matter tissue loss in the subcortical area, hippocampal fimbria, and striatum. Box-and-whiskers plots, with the box extending from the 25th to 75th percentiles and the median (line) depicted. The whiskers indicate the minimum and maximum values. The data were pooled from 4 independent experiments. Statistical analysis comparing the same brain region between the control and infected groups employed the Mann-Whitney test (**, $P < 0.01$; ***, $P < 0.001$). (C) Representative images of MAP-2- and MBP-stained sections at the hippocampus and striatum levels. Hemispheres ipsilateral to the carotid artery ligation are indicated with plus signs.

significantly further reduce the inflammation or affect the bacterial load in the infected animals ($n = 9$). When HI was combined with *S. epidermidis* infection, vancomycin treatment ($n = 30$) significantly reduced gray matter injury in the cortex, thalamus, and striatum, but not in the hippocampus (Fig. 6A), compared to saline-treated animals ($n = 21$). White matter injury in the striatum was also significantly reduced when SE-HI mice were treated with vancomycin. However, injury in the hippocampal fimbria was not reduced with the antibiotic treatment (Fig. 6B). Similar to the effects on inflammatory cytokines and the bacterial load, combining PTX with vancomycin ($n = 30$) did not provide further neuroprotection compared to vancomycin treatment alone.

Systemic *S. epidermidis* infection leads to transient perturbations in the brain.

To further investigate the mechanism of infection-potentiated HI brain injury, the blood-CSF barrier and blood-brain barrier (BBB) were examined for integrity after infection. *S. epidermidis* induced a modest number of leukocytes in the CSF at 6 h (23 ± 48 leukocytes/ μl of CSF; $n = 20$) and 14 h (13 ± 17 leukocytes/ μl ; $n = 11$), which was not different from saline-injected animals at 14 h (0 leukocytes/ μl ; $n = 5$; $P = 0.127$) and was similar to the level observed when *S. epidermidis* was injected into PND0 animals intravenously (24).

Under homeostatic conditions, sucrose entry into the brain is tightly regulated by the BBB. In *S. epidermidis*-infected animals, sucrose entry into the brain was significantly increased (Fig. 7A), suggesting the BBB integrity was modulated to permit augmented small-molecule blood-to-brain flux. Systemic inflammation induced by a high dose of lipopolysaccharide (LPS) can alter CBF in adult rats (25). Accordingly, we evaluated CBF upon *S. epidermidis* infection of mice and noted a trend toward reduced CBF in the infected animals that was not statistically significant (Fig. 7B).

To determine if *S. epidermidis* directly affects the brain, cytokine profiling of brain tissue homogenates was performed (Fig. 7C). Of the 23 cytokines tested, three, namely, CXCL1, CCL2, and G-CSF, were significantly upregulated in PND4-infected mice. Com-

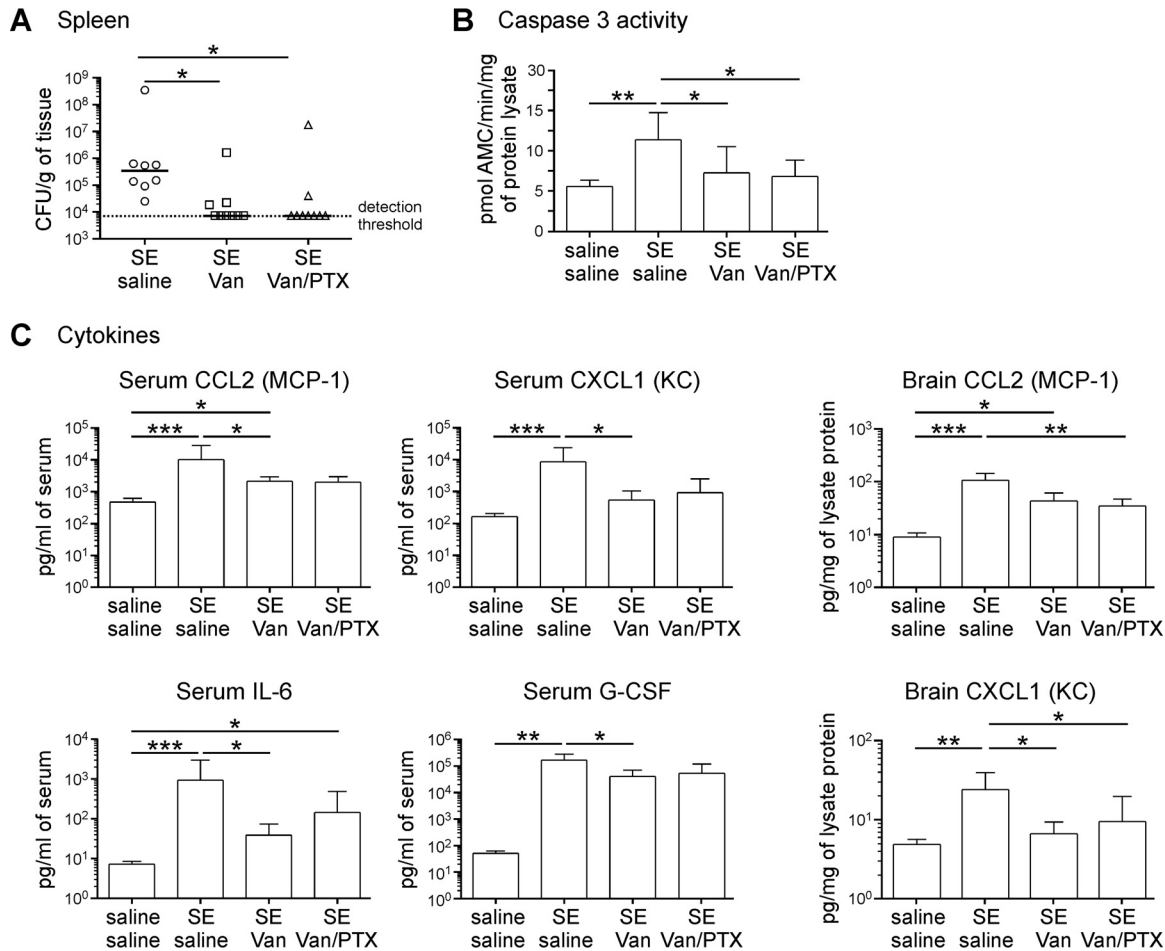


FIG 5 Vancomycin treatment reduced the bacterial load, peripheral inflammation, and caspase 3 activity in the brain. Mice i.p. injected with 3.5×10^7 CFU of *S. epidermidis* (SE) at PND4 were administered saline ($n = 9$), vancomycin (Van) ($n = 11$), or vancomycin with pentoxifylline (Van/PTX) ($n = 9$). Control mice were injected with saline only ($n = 6$). The mice were sacrificed for spleen CFU enumeration and cytokine analysis at 14 h postinfection. (A) Bacterial-cell counts in the spleen. The solid lines depict medians; the dotted line represents the detection threshold. (B) Caspase 3 activity analysis by cleavage of fluorometric substrates. The data are expressed as means plus SD. (C) Multiplex cytometric bead array analysis of cytokines in the serum and the brain. The data are expressed as means plus SD. The data were pooled from 3 independent experiments. Statistical analysis employed the Kruskal-Wallis test with Dunn's multiple-comparison *post hoc* test (*, $P < 0.05$; **, $P < 0.01$; ***, $P < 0.001$).

pared to the same cytokines detected in the peripheral blood, there was a lag in the production of cytokines in the brain, and peak levels were found between 14 and 24 h. Sepsis and inflammation can induce apoptotic cell death in the brain (26, 27). To determine if infection of PND4 mice via i.p. injection caused apoptotic events in the brain, the caspase 3 activity of brain lysates was measured (Fig. 7D). Following the time course of peripheral cytokine production, significant caspase 3 activity was observed at 14 and 24 h postinfection, which tapered back to basal levels by 48 h ($n = 7$ to 14 saline- and 10 to 12 *S. epidermidis*-injected mice per time point).

DISCUSSION

Infection and inflammation in newborns are well-established risk factors for neurological impairment. In this study, we demonstrate for the first time that infection with live *S. epidermidis* markedly increases the vulnerability of the preterm brain to HI-induced brain injury and that antibiotic treatment with vancomycin provides neuroprotection. Therapeutic hypothermia is the primary standard-of-care option in term neonates with HIE; however, the safety and efficacy of using hypothermia to treat even moderately preterm infants remain questionable (28). Moreover, as the etiology of brain injury in the preterm infant is likely different from that in the term infant (29),

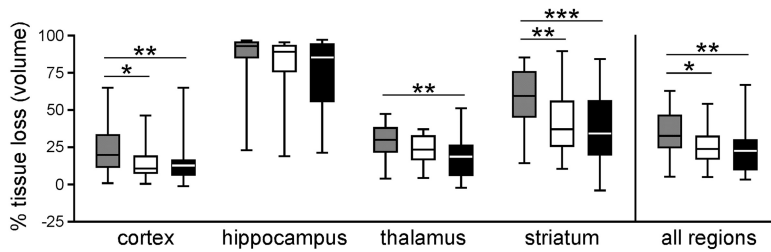
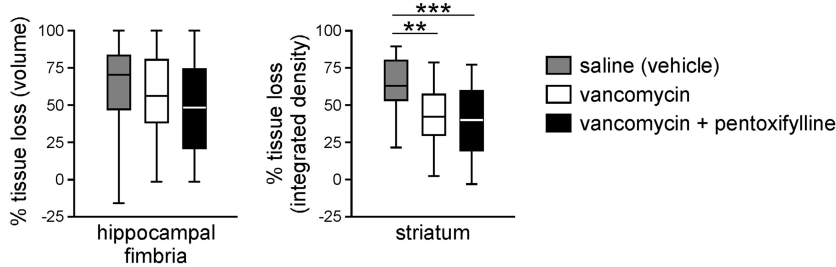
A Gray matter**B** White matter

FIG 6 Vancomycin treatment reduced potentiated hypoxic-ischemic brain injury in *S. epidermidis*-infected animals. Hypoxia-ischemia was induced 14 h after infection of PND4 mice with *S. epidermidis*. At the time of infection, mice were injected with saline ($n = 21$), vancomycin ($n = 30$), or vancomycin with pentoxifylline ($n = 30$). Brains were harvested 9 days later (on PND14), stained for microtubule-associated protein 2 or myelin basic protein, and analyzed for tissue loss in the ipsilateral hemisphere. Shown are percentages of gray matter (A) and white matter (B) tissue loss. Box-and-whiskers plots with the box extending from the 25th to 75th percentiles and the medians (line) are depicted. The whiskers indicate the minimum and maximum values. The data were pooled from 6 independent experiments. Statistical analysis comparing different treatment groups employed the Kruskal-Wallis test with Dunn's multiple-comparison *post hoc* test (*, $P < 0.05$; **, $P < 0.01$; ***, $P < 0.001$).

there is an unmet need for age-specific agents to prevent and/or treat preterm brain injury. Our newly developed neonatal model of live-bacterial infection combined with HI provides an important platform for testing novel neuroprotective therapies, which will help fill the current gap of lack of treatments for the vulnerable preterm population.

***S. epidermidis* infection model in neonatal mice.** Most studies investigating the interaction of staphylococci with the immune system have focused on *Staphylococcus aureus* (30). Although *S. epidermidis* causes a less pronounced inflammatory response than the more virulent *S. aureus*, infections with the commensal *S. epidermidis* are much more common in preterm infants (31, 32). Chemokines are the main proinflammatory mediators produced by human monocytes when activated by *S. aureus* or its constituents (33). Similarly, we found that *S. epidermidis* induced expression of multiple chemokines. Furthermore, several cytokines increased markedly in the blood, with IL-6 and IL-1 α demonstrating more than 10-fold increases upon *S. epidermidis* infection.

Although IL-6 plays a role in the maintenance of fever (34, 35), we did not observe temperature change in our infected animals. This was likely because mechanisms of thermoregulation are limited in neonatal pups (36), and their body temperature is maintained by nesting with the dam. In addition to temperature instability, weight loss is another clinical symptom of neonatal sepsis. The observed significant weight loss in our infected animals could be correlated with temporary loss of appetite and feeding (37), which also could partly explain the transient hypoglycemia observed in infected mice.

Cytokines released in the peripheral blood during an immune response can affect the endothelium, leading to vasodilation and capillary permeability, and in severe cases, such as sepsis-associated encephalopathy, the BBB can become dysfunctional (38). Indeed, we observed decreased integrity of the BBB, as well as a trend toward decreased CBF. Both of these factors may have contributed to the increased vulnera-

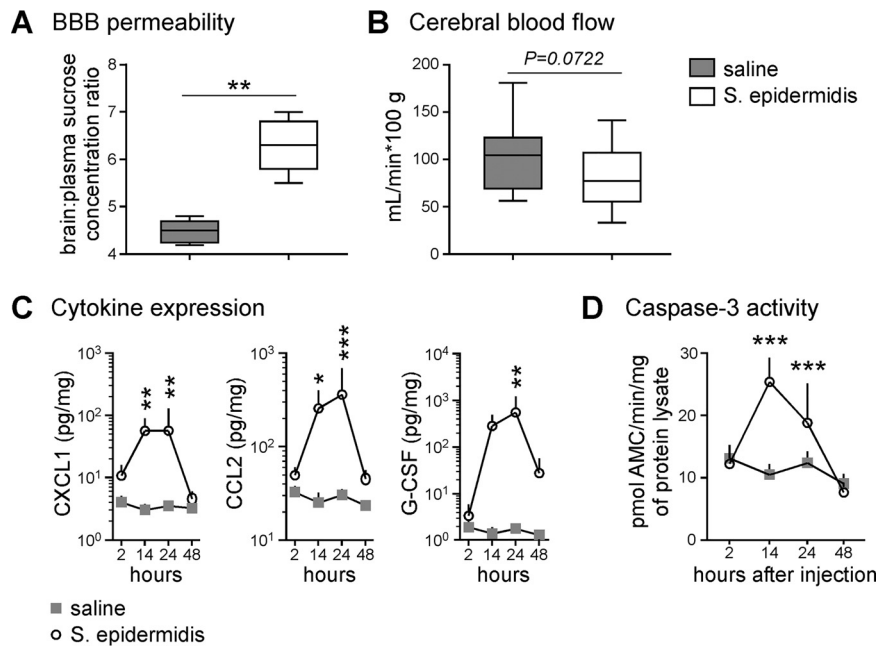


FIG 7 Perturbations in the brain after systemic *S. epidermidis* infection. (A) Blood-brain barrier permeability assay. [14 C]sucrose was administered to mice 14 hours after *S. epidermidis* or saline injection ($n = 5$ per group). Plasma and brain tissues were harvested 30 min later for scintillation counting. The data are expressed as the ratio between tissue and plasma scintillation counts (dots per minute). Box-and-whiskers plots with the box extending from the 25th to 75th percentiles and medians (lines) are depicted. The whiskers indicate the minimum and maximum values. Statistical analysis employed Student's *t* test (**, $P < 0.01$). (B) Cerebral blood flow assay. [14 C]iodoantipyrine was administered to mice 14 h after *S. epidermidis* ($n = 14$) or saline ($n = 15$) injection. Plasma and brain tissues were harvested 30 min later for scintillation counting. The data were pooled from two independent experiments. Statistical analysis employed Student's *t* test. (C and D) Mice were injected with saline or *S. epidermidis*. At various times postinfection, mice were sacrificed and perfused with saline, and brains were harvested for cytokine detection with a multiplex cytometric bead array (saline, $n = 6$; *S. epidermidis*, $n = 8$) (C) and caspase 3 activity analysis by cleavage of fluorometric substrates (saline, $n = 7$ to 14; *S. epidermidis*, $n = 10$ to 12) (D). Means plus SD are plotted. Statistical analysis employed two-way ANOVA with the Bonferroni *post hoc* test (*, $P < 0.05$; **, $P < 0.01$; ***, $P < 0.001$).

bility of the brain, as loss of BBB integrity can lead to vasogenic edema and brain swelling (39), and decreased CBF would add further to the ischemia during HI. Of the elevated inflammatory cytokines found in the periphery, only CCL2 and CXCL1 were found at increased levels in the brain. These cytokines were most likely produced by brain-resident cells or endothelial cells rather than crossing the BBB from the periphery (40). However, CCL2 can lead to BBB modulation (41), which could have contributed to the compromised BBB integrity observed.

Live bacteria compared to TLR agonists. We are the first to show that a transient systemic live-bacterial infection prior to HI exacerbates brain damage in neonatal mice. Previous studies employed synthetic or purified bacterial components or TLR agonists to induce inflammation (16–18, 23). Because cross talk of multiple TLRs and innate signaling pathways shapes the overall immune response, there are fundamental differences between using a single TLR agonist and using a live pathogen (42). *Escherichia coli* induces an immune response in neonatal rats different from that of LPS, a component of the Gram-negative bacterial cell wall that activates the TLR4 signaling pathway (43). Similarly, *S. epidermidis* can stimulate the TLR2 signaling pathway (44). Intact staphylococci can also activate other innate immune pathways through formylated peptide receptor, nucleotide-binding oligomerization domain (NOD) proteins, and TLR9 (45). Therefore, *S. epidermidis* infection is likely to activate multiple innate immune signaling pathways and to cause different changes in the animals than the synthetic bacterial lipopeptide TLR2 agonist Pam₃CSK₄. This is supported by our

previous observations that, while TLR2-deficient mice are protected from HI (17), brain pathology following *S. epidermidis* is not solely dependent on TLR2 (24).

We previously showed that Pam₃CSK₄ induces significant infiltration of leukocytes into the CSF of PND9 mice (46) and that the choroid plexus was the route of entry of immune cells from the periphery into the CSF (47). As *S. epidermidis* expresses multiple pathogen-associated molecular pattern (PAMP) molecules, including bacterial peptidoglycan and lipoteichoic acid, that can activate TLR2 (48, 49), we assessed whether *S. epidermidis* induces leukocyte infiltration in the CSF. In our PND4 mice, i.p. injection of *S. epidermidis* led to 100 times fewer leukocytes infiltrating into the CSF than when Pam₃CSK₄ was injected, but the degree of cell infiltration was similar to that in intravenously injected bacteria to PND0 animals (24). The different amounts of CSF-infiltrating cells may be due to the maturity of the immune system or the degree of innate TLR2 stimulation in the two different animal models. However, it should be noted that although Pam₃CSK₄, LPS, and *S. epidermidis* induced similar peripheral cytokine responses, only Pam₃CSK₄ led to a significant influx of leukocytes into the CSF, suggesting that the peripheral inflammatory response *per se* is not the determining factor (46). In addition to using potentially nonphysiological doses when employing a synthetic TLR ligand, our data suggest that live *S. epidermidis* induces an immune response different from that to Pam₃CSK₄, supporting the notion that it is important to use actual pathogens rather than purified TLR agonists in animal models.

Similar models of live-bacterial infection or inflammation. A previous study showed that intravenous injection of *S. epidermidis* in PND0 pups caused reductions in the gray and white matter (24). However, in our model, when bacteria were i.p. injected into PND4 mice, no gross changes in the brain tissue were observed. This difference could be due to the age of the animals and the route of infection, as well as the dose of the inoculum. For example, LPS causes white matter changes only when injected into mice at PND1 or -2, but not at PND3 or later (50). Nevertheless, transient molecular perturbations, including chemokine production and caspase activation, as well as physiological changes in the brain, were observed in our infected PND4 animals, similar to observations previously made in PND0 animals (24).

Decreasing inflammation as a neuroprotective strategy. In this model of HI brain injury, a live-bacterial infection was used to induce inflammation, and we therefore investigated if antibiotics are beneficial for suppressing the potentiated brain injury. In the context of *E. coli* infection and treatment with beta-lactam antibiotics, antibiotic-induced endotoxin release can lead to septic shock (51); it is therefore possible that using the bacterial-cell-wall-active glycopeptide bactericidal antibiotic vancomycin would induce release of bacterial constituents, leading to a spike in inflammation, further exacerbating the HI brain injury. While a single dose of vancomycin did not completely eliminate the bacteria, vancomycin reduced brain damage in the cortex, striatum, and midbrain of *S. epidermidis*-infected animals experiencing an episode of HI. Although the dose of vancomycin used in this experiment was not enough to eliminate the bacterial infection, the outcome of the vancomycin treatment may merely be due to the bactericidal effects leading to an overall reduction of the bacterial load and associated inflammation in the animals at the time of HI. However, since vancomycin can specifically inhibit LPS-induced tumor necrosis factor alpha (TNF- α) (52) but stimulate IL-10 production (53), this suggests that vancomycin might also shift the pattern of cytokine release to an anti-inflammatory profile.

We also evaluated the immunomodulating drug PTX as an adjunct therapy to vancomycin to further suppress inflammation with the final goal of further decreasing HI brain injury. In this experimental model, we found that coadministration of PTX with vancomycin did not further suppress inflammation, consistent with a recent *in vitro* study in which PTX was more effective at inhibiting inflammation induced by *E. coli* than that induced by *S. epidermidis* (54). Consistent with the lack of adjunct effects of PTX on *S. epidermidis*-induced inflammation, administration of PTX with vancomycin

did not provide further neuroprotection in our SE-HI model compared to using vancomycin alone.

Limitations of the study. Our animal model of combined bacterial infection and HI resulted in severe injury in the hippocampus, which may have limited the neuroprotective effects in this region. By reducing the hypoxia period and thereby decreasing the injury, neuroprotection may also have been achieved in this brain region. The study has some limitations, including the following: (i) innate immune responses may be species specific, (ii) the timing of antibiotic and anti-inflammatory agent administration may substantially affect outcomes, and (iii) the timing of the infection with respect to the HI insult varies case by case clinically and can occur after the HI insult.

Innate immune response differences between humans and rodents have long been observed. Pertinent to this study, TLR2 expression on murine blood cells is strongly inducible, whereas human TLR2 is constitutively expressed (55). Human and mouse physiologies are influenced by the microbiome, and specifically, *S. epidermidis* is not part of the normal flora in mice (56). These confounding factors affect our mouse model's ability to fully reflect human immune responses upon *S. epidermidis* infection.

Conclusions. Overall, our study has multiple strengths, including (i) establishment of a novel *in vivo* model of *S. epidermidis* infection that triggers systemic inflammation and preterm brain injury, (ii) use of a clinically relevant live bacterial pathogen, (iii) demonstrating that the antibiotic vancomycin can reduce *S. epidermidis*-potentiated HI brain injury, and (iv) evaluation of a candidate adjunctive agent, PTX. Although there are limitations, we present evidence that decreasing the bacterial load and inflammation with the use of antibiotics is beneficial for alleviating brain injury in newborn mice.

MATERIALS AND METHODS

Animals. Six- to 8-week-old C57BL/6 mice purchased from Janvier Laboratories (Le Genest-Saint-Isle, France) and Charles River Laboratories (Sulzfeld, Germany) were bred at the Laboratory for Experimental Biomedicine (University of Gothenburg, Gothenburg, Sweden). Paired breeders were housed in single cages with a 12-h light-dark cycle with free access to food and water. The day of birth was defined as PND0. The median weight for PND4 animals was 2.5 g. All animal studies were performed in accordance with the ethical standards of the University of Gothenburg and in accordance with protocols approved by the Gothenburg Animal Ethics Committee (no. 18/2015 and 633/2017). Unless otherwise stated, experiments were performed independently at least 3 times, using animals from at least 3 different litters, with a minimum of 2 or 3 animals from each litter in each treatment group.

Bacterial inoculum preparation. *S. epidermidis* 1457, an invasive clinical strain obtained from an adult patient with a central venous catheter infection, was a kind gift from Michael Otto's laboratory (57). A mid-log-phase bacterial culture was mixed with 50% glycerol at a 1:1 ratio and stored at -80°C . On the day of infection, 15 μl of an overnight culture prepared from the frozen stock was added to 15 ml of tryptic soy broth (Corning; 46-060-CI; Fisher Scientific, Sweden) in a 125-ml vented Erlenmeyer flask and shaken for approximately 4 h at 37°C and 240 rpm (MaxQ 4450 benchtop orbital shaker; Thermo Scientific, Sweden). The optical density (OD) of the bacterial culture at 600 nm was measured with a Spectramax Plus spectrophotometer (Molecular Devices) to ensure an exponential growth phase between OD 0.3 and 0.4 was reached. The density of the bacteria was calculated using a conversion factor of 2.975×10^8 CFU/ml per OD unit. The culture (12 ml) was centrifuged at $3,000 \times g$ for 5 min at 4°C and then resuspended in endotoxin-free saline (Sigma-Aldrich, Sweden) at 5×10^8 or 1.75×10^9 CFU/ml for injection. For each experiment, retrospective confirmation of the correct inoculum dose and a check for contaminating microorganisms were performed by spread plating on tryptic soy agar plates (Sigma-Aldrich) and incubating at 37°C overnight.

To generate the OD-to-CFU per milliliter conversion factor, mid-log-phase bacterial cultures were sampled for CFU enumeration by spread plating, while the OD measurement was taken simultaneously. A conversion factor based on the slope of the CFU per milliliter-versus-OD plot was used initially and was later adjusted based on retrospective spread-plating results to account for errors due to the centrifugation and resuspension steps.

Infection and hypoxia-ischemia model and sample preparation. Animals, independently of sex, were ranked according to body weight and then assigned in equal numbers to different treatment groups to reduce experimental bias. Pups were intraperitoneally injected with a sublethal dose of *S. epidermidis* (1×10^7 or 3.5×10^7 CFU in 20 μl of saline) at PND4 or -5. The age of *S. epidermidis* administration was chosen to mirror a stage in murine brain development equivalent to the preterm human (58).

At 2, 14, 24, or 48 h postinfection, mice were euthanized via i.p. administration of pentobarbital (Pentacour). Blood was collected via cardiac puncture for serum analysis or mixed with EDTA to a final concentration of 12 mM for bacterial CFU enumeration. The animals were then perfused intracardially with saline, and the spleens were collected in 100 μl of ice-cold saline. Brains were flash frozen on dry ice and stored at -80°C until lysate preparation 2 to 7 weeks later. Brain lysates were prepared by first

homogenizing the brain in phosphate-buffered saline (PBS) with a pellet mixer (VWR, Spånga, Sweden) and then sonicating it in homogenization buffer (5 mM EDTA, 1% Triton X-100, PBS) containing 1% protease inhibitor cocktail (Sigma-Aldrich; P8340), with centrifugation at $10,000 \times g$ for 10 min at 4°C for clearance. The cleared lysates were aliquoted and stored at -80°C until analysis the next day. In certain experiments, CSF was sampled from euthanized mice and analyzed for bacterial CFU enumeration or leukocyte infiltration as described previously (24).

For the combined bacterial infection and HI (SE-HI) model, HI procedures were performed as described previously (59). In brief, the left common carotid artery was ligated at 12 h postinfection and then, at 14 h postinfection, exposed to 10% O₂ for 60 min. Mice were sacrificed 9 days later (PND14) for analysis of the brain pathology. In some experiments, pentoxifylline (Sigma-Aldrich; P1784) and vancomycin (Sigma-Aldrich; V8138), dissolved in saline and filter sterilized, were i.p. injected into mice 2 min after the injection of bacteria (at a site contralateral to the bacterial injection site) at 40 and 15 mg/kg of body weight, respectively. The pentoxifylline dose was based on what was shown in previous studies to provide neuroprotection in rats (15) but not causing morbidity in infected neonatal mice (60). The vancomycin dose was determined based on a previous neonatal infection model (61) and trial experiments that led to reduction, but not elimination, of the bacterial load in infected animals. Drugs or vehicle were randomly assigned to the pups after body weight ranking. Due to high biological variation, the average number of animals used for the HI brain injury model was 15 to 20 (59, 62). Factoring in variations in response to bacteria and therapeutic drugs, we used between 20 and 30 animals for each treatment group.

Bacterial enumeration. Splens in saline were homogenized with a pellet mixer and serially diluted with saline for plating and CFU enumeration. Samples from infected mice were spot plated (10 μl per spot) onto tryptic soy agar plates in duplicate. The spots with countable colonies between 9 and 60 CFU were used to calculate the number of CFU per gram of tissue. Samples from control (saline-injected) animals were spread plated (100 μl) on tryptic soy agar plates. The detection threshold of bacteria in the spleen was 7,300 CFU/g of tissue.

EDTA-treated blood (5 or 10 μl) was spread on tryptic soy agar for CFU enumeration. With 9 CFU being the lower limit for plate counting, spread plating 5 μl (for the 2-, 14-, and 24-h time points) and 10 μl (for the 2-, 3-, and 5-day time points) of blood corresponded to detection thresholds of 1,000 and 2,000 CFU/ml of blood, respectively.

Physiological measurements. Rectal temperatures were measured with a thermistor microprobe (BAT-12; Physitemp Instruments, Clifton, NJ, USA). Pups were removed from their dams in a randomized order, and the microprobe lubricated with petroleum jelly was inserted into each animal for temperature recording (one measurement per animal). The procedure was performed quickly on the entire litter to prevent a significant body temperature drop. Body temperature was measured at 2, 6, 14, 24, and 48 h postinfection. The body weights of the animals were measured at 24, 48, and 72 h and at 5, 8, and 10 days postinfection. Cytokines in sera and brain lysates were detected with a cytometric bead array using the Bio-Plex Pro mouse cytokine 23-plex assay (Bio-Rad) and analyzed with the Luminex 200 system (Bio-Rad) according to the manufacturer's instructions. Trunk blood plasma collected by decapitation of the animal was used for glucose measurements with an Accu-chek Compact Plus blood glucose monitor (Roche).

Assessment of brain injury. Brain tissue processing and immunohistochemistry procedures were performed as previously described (63). Seven-micrometer-thick coronal sections were cut at 6 brain levels, 50 sections apart, and stained for microtubule-associated protein 2 (MAP-2) or myelin basic protein (MBP). Images of the stained sections were analyzed with ImageJ (NIH), with the experimenter blinded to the animal identities. The functions area, length, and mean gray value (pixel intensity) were used to make measurements within a highlighted region of interest (ROI). The integrated density was calculated as the area within the ROI times the mean gray value of the ROI. The MAP-2-stained areas of the cortex (6 levels), hippocampus (3 levels), thalamus (3 levels), and striatum (4 or 5 levels) were measured. The MBP-stained area of the hippocampal fimbria (2 or 3 levels), the area of subcortical white matter dorsal to the hippocampus (2 or 3 levels), the thickness of the corpus callosum (4 levels), and the integrated density of the striatum (3 levels) were measured. Volumes were calculated according to the Cavalieri principle using the following equation: $V = \Sigma A \div P \times T$, where V is the total volume, ΣA is the sum of the areas measured, P is the sampling fraction, and T is the section thickness. Tissue loss in the ipsilateral hemisphere was calculated as a percentage of the contralateral hemisphere: $(\text{contralateral} - \text{ipsilateral}) \div \text{contralateral} \times 100\%$.

Blood-brain barrier permeability and cerebral blood flow assays. Assessments of BBB permeability were performed 14 h after saline or *S. epidermidis* injection in PND4 animals. The animals were injected with [¹⁴C]sucrose intraperitoneally (600 mCi/mmol; 0.3 μCi/g of body weight; American Radio-labeled Chemical, Saint Louis, MO, USA) and sacrificed 30 min later by pentobarbital injection. Blood samples were mixed with EDTA, while brain regions were dissected out and dissolved in Soluene 350 (PerkinElmer), and isotope activity in each tissue or blood plasma sample was determined by liquid scintillation counting. Brain/plasma sucrose concentration ratios were used as a measure of blood-brain permeability as previously described (64). For CBF analysis, 3 μCi of 4-iodo[*N*-methyl-¹⁴C]antipyrine in 30 μl of saline was injected subcutaneously. The animals were sacrificed 30 s later by decapitation. Brain and blood samples were collected as described above, and CBF calculations were performed as previously described (64). Due to the high sensitivity and low variation of the assay, the BBB permeability assay was performed once, and CBF was analyzed in two independent experiments.

Caspase 3 activity measurement. The caspase 3 activities of cleared brain lysates were measured by the cleavage rate of acetyl-Asp-Glu-Val-Asp-α-(4-methylcoumaryl-7-amide) peptide substrate (Peptide Institute; no. 3171-v) at 37°C using a SpectraMax Gemini fluorometer (Molecular Devices) as previously

described (27, 64). The protein concentrations of the cleared lysates were determined using a bicinchoninic acid protein assay kit (Sigma-Aldrich) according to the manufacturer's instructions.

Statistics. After testing for normality and variance, nonparametric tests were selected for statistical analyses of brain histology data. A Mann-Whitney U test or one-way analysis of variance (ANOVA) using the Kruskal-Wallis test with Dunn's multiple comparisons was employed. For analysis of physiological data (cytokines, body temperature, blood glucose, and CBF), where data showed Gaussian distribution, 2-way ANOVA or two-way repeated-measures ANOVA with the Bonferroni *post hoc* test was employed.

SUPPLEMENTAL MATERIAL

Supplemental material is available online only.

SUPPLEMENTAL FILE 1, PDF file, 0.2 MB.

ACKNOWLEDGMENTS

We thank Zineb Chaabi, Anna-Lena Leverin, and Anna-Jean Mallard for technical support.

The study was conceived and designed by J.C.Y.L., X.W., O.L., A.C., T.S., and C.M. Experiments were performed by J.C.Y.L., P.S., C.J.E., and A.M. J.C.Y.L. and C.M. drafted the manuscript. We all critically reviewed and edited the work.

We declare no competing financial interests.

The work was funded by Vinnova Vinnmer Marie-Curie Incoming (2015-01505; J.C.Y.L.), the Wilhelm and Martina Lundgrens Foundation (2016-1323, 2017-1966, and 2018-2465, J.C.Y.L.; 2017-1911 and 2018-2368, C.J.E.), the Lilla Barnets Fund (20170806; J.C.Y.L., C.M., and C.J.E.), the Anna-Brita and Bo Castegrens Memorial Foundation (LA2017-0269; J.C.Y.L.), the Swedish Research Council (VR-2017-01409, C.M.; VR-2018-02682, X.W.), the ALF Agreement (ALFGBG-722491, C.M.; ALFGBG-813291, X.W.), the Leducq Foundation (DSRR_P34404; C.M.), the Swedish Brain Foundation (FO2017-0063, C.M.; F018-0090, X.W.), the Torsten Söderberg Foundation (M98/15; C.M.), the Åhlen Foundation (C.M.), the Cerebral Palsy Alliance Australia (PG4416; C.J.E.), the Stroke-Riksförbundet (C.J.E.), and the Telethon Perth Children's Hospital Research Funds (T.S. and A.C.).

REFERENCES

- Manuck TA, Rice MM, Bailit JL, Grobman WA, Reddy UM, Wapner RJ, Thorp JM, Caritis SN, Prasad M, Tita ATN, Saade GR, Sorokin Y, Rouse DJ, Blackwell SC, Tolosa JE, Varner M, Hill K, Sowles A, Postma J, Alexander S, Andersen G, Scott V, Morby V, Jolley K, Miller J, Berg B, Talucci M, Zylfijaj M, Reid Z, Leed R, Benson J, Forester S, Kitto C, Davis S, Falk M, Perez C, Dorman K, Mitchell J, Kaluta E, Clark K, Spicer K, Timlin S, Wilson K, Leveno K, Moseley L, Santillan M, Price J, Buentipo K, Bludau V, Thomas T, Fay L, Melton C, Kingsbery J, Benezue R, Simhan H, Bickus M, Fischer D, Kamon T, Deangelis D, Mercer B, Milluzzi C, Dalton W, Dotson T, McDonald P, Brezine C, McGrail A, Latimer C, Guzzo L, Johnson F, Gerwig L, Fyffe S, Loux D, Frantz S, Cline D, Wylie S, Iams J, Wallace M, Northen A, Grant J, Colquitt C, Rouse D, Andrews W, Mallett G, Ramos-Brinson M, Roy A, Stein L, Campbell P, Collins C, Jackson N, Dinsmoor M, Senka J, Paychek K, Peaceman A, Moss J, Salazar A, Acosta A, Hankins G, Hauff N, Palmer L, Lockhart P, Driscoll D, Wynn L, Sudz C, Dengate D, Girard C, Field S, Breault P, Smith F, Annunziata N, Allard D, Silva J, Gamage M, Hunt J, Tillinghast J, Corcoran N, Jimenez M, Ortiz F, Givens P, Rech B, Moran C, Hutchinson M, Spears Z, Carreno C, Heaps B, Zamora G, Seguin J, Rincon M, Snyder J, Farrar C, Lairson E, Bonino C, Smith W, Beach K, Van Dyke S, Butcher S, Thom E, Zhao Y, McGee P, Momirova V, Palugod R, Reamer B, Larsen M, Williams T, Spangler T, Lozitska A, Spong C, Tolivaisa S, Vandersten JP. 2016. Preterm neonatal morbidity, and mortality by gestational age: a contemporary cohort. *Am J Obstet Gynecol* 215:103.e1–103.e14. <https://doi.org/10.1016/j.ajog.2016.01.004>.
- Strunk T, Inder T, Wang X, Burgner D, Mallard C, Levy O. 2014. Infection-induced inflammation and cerebral injury in preterm infants. *Lancet Infect Dis* 14:751–762. [https://doi.org/10.1016/S1473-3099\(14\)70710-8](https://doi.org/10.1016/S1473-3099(14)70710-8).
- Galinsky R, Lear CA, Dean JM, Wassink G, Dhillon SK, Fraser M, Davidson JO, Bennet L, Gunn AJ. 2018. Complex interactions between hypoxia-ischemia and inflammation in preterm brain injury. *Dev Med Child Neurol* 60:126–133. <https://doi.org/10.1111/dmcn.13629>.
- Dong Y, Speer CP. 2015. Late-onset neonatal sepsis: recent developments. *Arch Dis Child Fetal Neonatal Ed* 100:F257–F263. <https://doi.org/10.1136/archdischild-2014-306213>.
- Marchant EA, Boyce GK, Sadarangani M, Lavoie PM. 2013. Neonatal sepsis due to coagulase-negative staphylococci. *Clin Dev Immunol* 2013: 586076. <https://doi.org/10.1155/2013/586076>.
- Derienzo C, Kohler JA, Lada E, Meanor P, Tanaka D. 2016. Demonstrating the relationships of length of stay, cost and clinical outcomes in a simulated NICU. *J Perinatol* 36:1128–1131. <https://doi.org/10.1038/jp.2016.128>.
- Buttner H, Mack D, Rohde H. 2015. Structural basis of *Staphylococcus epidermidis* biofilm formation: mechanisms and molecular interactions. *Front Cell Infect Microbiol* 5:14. <https://doi.org/10.3389/fcimb.2015.00014>.
- Schüller SS, Kramer BW, Villamor E, Spittler A, Berger A, Levy O. 2018. Immunomodulation to prevent or treat neonatal sepsis: past, present, and future. *Front Pediatr* 6:199. <https://doi.org/10.3389/fped.2018.00199>.
- Pammi M, Haque KN. 2015. Pentoxifylline for treatment of sepsis and necrotizing enterocolitis in neonates. *Cochrane Database Syst Rev* 4:CD004205. <https://doi.org/10.1002/14651858.CD004205.pub3>.
- Hamilçikan Ş, Can E, Büke Ö, Erol M, Gayret ÖB. 2017. Pentoxifylline treatment of very low birth weight neonates with nosocomial sepsis. *Am J Perinatol* 34:795–800. <https://doi.org/10.1055/s-0037-1598596>.
- Pammi M, Haque KN. 2015. Pentoxifylline for treatment of sepsis and necrotizing enterocolitis in neonates. *Cochrane Database Syst Rev* 3:CD004205. <https://doi.org/10.1002/14651858.CD004205.pub3>.
- Bowton DL, Stump DA, Prough DS, Toole JF, Lefkowitz DS, Coker L. 1989. Pentoxifylline increases cerebral blood flow in patients with cerebrovascular disease. *Stroke* 20:1662–1666. <https://doi.org/10.1161/01.str.20.12.1662>.
- Kalay S, Oztekin O, Tezel G, Aldemir H, Sahin E, Koksoy S, Akcakus M, Oygur N. 2013. The effects of intraperitoneal pentoxifylline treatment in

- rat pups with hypoxic-ischemic encephalopathy. *Pediatr Neurol* 49: 319–323. <https://doi.org/10.1016/j.pediatrneurol.2013.05.011>.
14. Dilek M, Kumral A, Okyay E, Ozbal S, Tugyan K, Tuzun F, Sever AH, Yilmaz O, Duman N, Ozkan H. 2013. Protective effects of pentoxifylline on lipopolysaccharide-induced white matter injury in a rat model of periventricular leukomalacia. *J Matern Fetal Neonatal Med* 26: 1865–1871. <https://doi.org/10.3109/14767058.2013.798290>.
 15. Eun BL, Liu XH, Barks JD. 2000. Pentoxifylline attenuates hypoxic-ischemic brain injury in immature rats. *Pediatr Res* 47:73–78. <https://doi.org/10.1203/00006450-200001000-00014>.
 16. Stridh L, Mottahedin A, Johansson ME, Valdez RC, Northington F, Wang X, Mallard C. 2013. Toll-like receptor-3 activation increases the vulnerability of the neonatal brain to hypoxia-ischemia. *J Neurosci* 33: 12041–12051. <https://doi.org/10.1523/JNEUROSCI.0673-13.2013>.
 17. Mottahedin A, Svedin P, Nair S, Mohn CJ, Wang X, Hagberg H, Ek J, Mallard C. 2017. Systemic activation of Toll-like receptor 2 suppresses mitochondrial respiration and exacerbates hypoxic-ischemic injury in the developing brain. *J Cereb Blood Flow Metab* 37:1192–1198. <https://doi.org/10.1177/0271678X17691292>.
 18. Wang X, Stridh L, Li W, Dean J, Elmghren A, Gan L, Eriksson K, Hagberg H, Mallard C. 2009. Lipopolysaccharide sensitizes neonatal hypoxic-ischemic brain injury in a MyD88-dependent manner. *J Immunol* 183: 7471–7477. <https://doi.org/10.4049/jimmunol.0900762>.
 19. Mallard C, Vexler ZS. 2015. Modeling ischemia in the immature brain: How translational are animal models? *Stroke* 46:3006–3011. <https://doi.org/10.1161/STROKEAHA.115.007776>.
 20. Semple BD, Blomgren K, Gimlin K, Ferriero DM, Noble-Haeusslein LJ. 2013. Brain development in rodents and humans: identifying benchmarks of maturation and vulnerability to injury across species. *Prog Neurobiol* 106–107:1–16. <https://doi.org/10.1016/j.pneurobio.2013.04.001>.
 21. Marco AJ, Domingo M, Ruberte J, Carretero A, Briones V, Dominguez L. 1992. Lymphatic drainage of *Listeria monocytogenes* and Indian ink inoculated in the peritoneal cavity of the mouse. *Lab Anim* 26:200–205. <https://doi.org/10.1258/002367792780740549>.
 22. Lukas G, Brindle SD, Greengard P. 1971. The route of absorption of intraperitoneally administered compounds. *J Pharmacol Exp Ther* 178: 562–564.
 23. Eklind S, Mallard C, Arvidsson P, Hagberg H. 2005. Lipopolysaccharide induces both a primary and a secondary phase of sensitization in the developing rat brain. *Pediatr Res* 58:112–116. <https://doi.org/10.1203/01.PDR.0000163513.03619.8D>.
 24. Bi D, Qiao L, Bergelson I, Ek CJ, Duan L, Zhang X, Albertsson AM, Pettengill M, Kronforst K, Ninkovic J, Goldmann D, Janzon A, Hagberg H, Wang X, Mallard C, Levy O. 2015. Staphylococcus epidermidis bacteremia induces brain injury in neonatal mice via Toll-like receptor 2-dependent and -independent pathways. *J Infect Dis* 212:1480–1490. <https://doi.org/10.1093/infdis/jiv231>.
 25. Semmler A, Okulla T, Sastre M, Dumitrescu-Ozimek L, Heneka MT. 2005. Systemic inflammation induces apoptosis with variable vulnerability of different brain regions. *J Chem Neuroanat* 30:144–157. <https://doi.org/10.1016/j.jchemneu.2005.07.003>.
 26. Kafa IM, Uysal M, Bakirci S, Kurt A. 2010. Sepsis induces apoptotic cell death in different regions of the brain in a rat model of sepsis. *Acta Neurobiol Exp* 70:246–260.
 27. Wang X, Karlsson JO, Zhu C, Bahr BA, Hagberg H, Blomgren K. 2001. Caspase-3 activation after neonatal rat cerebral hypoxia-ischemia. *Biol Neonate* 79:172–179. <https://doi.org/10.1159/000047087>.
 28. Rao R, Trivedi S, Vesoulis Z, Liao SM, Smyser CD, Mathur AM. 2017. Safety and short-term outcomes of therapeutic hypothermia in preterm neonates 34–35 weeks gestational age with hypoxic-ischemic encephalopathy. *J Pediatr* 183:37–42. <https://doi.org/10.1016/j.jpeds.2016.11.019>.
 29. Gopagondanahalli KR, Li J, Fahey MC, Hunt RW, Jenkin G, Miller SL, Malhotra A. 2016. Preterm hypoxic-ischemic encephalopathy. *Front Pediatr* 4:114. <https://doi.org/10.3389/fped.2016.00114>.
 30. Vuong C, Otto M. 2002. Staphylococcus epidermidis infections. *Microbes Infect* 4:481–489. [https://doi.org/10.1016/s1286-4579\(02\)01563-0](https://doi.org/10.1016/s1286-4579(02)01563-0).
 31. Zea-Vera A, Ochoa TJ. 2015. Challenges in the diagnosis and management of neonatal sepsis. *J Trop Pediatr* 61:1–13. <https://doi.org/10.1093/tropej/fmu079>.
 32. Yusef D, Shalakhti T, Awad S, Algharaibeh H, Khasawneh W. 2018. Clinical characteristics and epidemiology of sepsis in the neonatal intensive care unit in the era of multi-drug resistant organisms: a retrospective review. *Pediatr Neonatol* 59:35–41. <https://doi.org/10.1016/j.pedneo.2017.06.001>.
 33. Wang ZM, Liu C, Dziarski R. 2000. Chemokines are the main proinflammatory mediators in human monocytes activated by Staphylococcus aureus, peptidoglycan, and endotoxin. *J Biol Chem* 275:20260–20267. <https://doi.org/10.1074/jbc.M909168199>.
 34. Cartmell T, Poole S, Turnbull AV, Rothwell NJ, Luheshi GN. 2000. Circulating interleukin-6 mediates the febrile response to localised inflammation in rats. *J Physiol* 526:653–661. <https://doi.org/10.1111/j.1469-7793.2000.00653.x>.
 35. Eskilsson A, Mirrasekhan E, Dufour S, Schwanager M, Engblom D, Blomqvist A. 2014. Immune-induced fever is mediated by IL-6 receptors on brain endothelial cells coupled to STAT3-dependent induction of brain endothelial prostaglandin synthesis. *J Neurosci* 34:15957–15961. <https://doi.org/10.1523/JNEUROSCI.3520-14.2014>.
 36. Nagy ZM. 1993. Development of homeothermy in infant C3H mice. *Bull Psychon Soc* 31:221–224. <https://doi.org/10.3758/BF03337329>.
 37. Granger JL, Ratti PL, Datta SC, Raymond RM, Opp MR. 2013. Sepsis-induced morbidity in mice: effects on body temperature, body weight, cage activity, social behavior and cytokines in brain. *Psychoneuroendocrinology* 38:1047–1057. <https://doi.org/10.1016/j.psychoneu.2012.10.010>.
 38. Kuperberg SJ, Wadgaonkar R. 2017. Sepsis-associated encephalopathy: the blood-brain barrier and the sphingolipid rheostat. *Front Immunol* 8:597. <https://doi.org/10.3389/fimmu.2017.00597>.
 39. Vannucci RC, Christensen MA, Yager JY. 1993. Nature, time-course, and extent of cerebral edema in perinatal hypoxic-ischemic brain damage. *Pediatr Neurol* 9:29–34. [https://doi.org/10.1016/0887-8994\(93\)90006-x](https://doi.org/10.1016/0887-8994(93)90006-x).
 40. Pan W, Stone KP, Hsueh H, Manda VK, Zhang Y, Kastin AJ. 2011. Cytokine signaling modulates blood-brain barrier function. *Curr Pharm Des* 17:3729–3740. <https://doi.org/10.2174/138161211798220918>.
 41. Stamatovic SM, Keep RF, Kunkel SL, Andjelkovic AV. 2003. Potential role of MCP-1 in endothelial cell tight junction “opening”: signaling via Rho and Rho kinase. *J Cell Sci* 116:4615–4628. <https://doi.org/10.1242/jcs.00755>.
 42. Tan RS, Ho B, Leung BP, Ding JL. 2014. TLR cross-talk confers specificity to innate immunity. *Int Rev Immunol* 33:443–453. <https://doi.org/10.3109/08830185.2014.921164>.
 43. Schwarz JM, Bilbo SD. 2011. LPS elicits a much larger and broader inflammatory response than *Escherichia coli* infection within the hippocampus of neonatal rats. *Neurosci Lett* 497:110–115. <https://doi.org/10.1016/j.neulet.2011.04.042>.
 44. Strunk T, Power Coombs MR, Currie AJ, Richmond P, Golenbock DT, Stoler-Barak L, Gallington LC, Otto M, Burgner D, Levy O. 2010. TLR2 mediates recognition of live Staphylococcus epidermidis and clearance of bacteremia. *PLoS One* 5:e10111. <https://doi.org/10.1371/journal.pone.0010111>.
 45. Fournier B, Philpott DJ. 2005. Recognition of Staphylococcus aureus by the innate immune system. *Clin Microbiol Rev* 18:521–540. <https://doi.org/10.1128/CMR.18.3.521-540.2005>.
 46. Mottahedin A, Smith PL, Hagberg H, Ek CJ, Mallard C. 2017. TLR2-mediated leukocyte trafficking to the developing brain. *J Leukoc Biol* 101:297–305. <https://doi.org/10.1189/jlb.3A1215-568R>.
 47. Mottahedin A, Joakim Ek C, Truvé K, Hagberg H, Mallard C. 2019. Choroid plexus transcriptome and ultrastructure analysis reveals a TLR2-specific chemotaxis signature and cytoskeleton remodeling in leukocyte trafficking. *Brain Behav Immun* 79:216–227. <https://doi.org/10.1016/j.bbi.2019.02.004>.
 48. Schwandner R, Dziarski R, Wesche H, Rothe M, Kirschning CJ. 1999. Peptidoglycan- and lipoteichoic acid-induced cell activation is mediated by Toll-like receptor 2. *J Biol Chem* 274:17406–17409. <https://doi.org/10.1074/jbc.274.25.17406>.
 49. Lai Y, Cogen AL, Radek KA, Park HJ, Macleod DT, Leightle A, Ryan AF, Di Nardo A, Gallo RL. 2010. Activation of TLR2 by a small molecule produced by Staphylococcus epidermidis increases antimicrobial defense against bacterial skin infections. *J Invest Dermatol* 130:2211–2221. <https://doi.org/10.1038/jid.2010.123>.
 50. Nobuta H, Ghiani CA, Paez PM, Spreuer V, Dong H, Korsak RA, Manukyan A, Li J, Vinters HV, Huang EJ, Rowitch DH, Sofroniew MV, Campagnoni AT, De Vellis J, Waschek JA. 2012. STAT3-mediated astrogliosis protects myelin development in neonatal brain injury. *Ann Neurol* 72:750–765. <https://doi.org/10.1002/ana.23670>.
 51. Lepper PM, Held TK, Schneider EM, Bölke E, Gerlach H, Trautmann M. 2002. Clinical implications of antibiotic-induced endotoxin release in

- septic shock. *Intensive Care Med* 28:824–833. <https://doi.org/10.1007/s00134-002-1330-6>.
52. Siedlar M, Szczepanik A, Wieckiewicz J, Pituch-Noworolska A, Zembala M. 1997. Vancomycin down-regulates lipopolysaccharide-induced tumour necrosis factor alpha (TNF alpha) production and TNF alpha-mRNA accumulation in human blood monocytes. *Immunopharmacology* 35: 265–271. [https://doi.org/10.1016/s0162-3109\(96\)00156-7](https://doi.org/10.1016/s0162-3109(96)00156-7).
53. Ziegeler S, Raddatz A, Hoff G, Buchinger H, Bauer I, Stockhausen A, Sasse H, Sandmann I, Hörsch S, Rensing H. 2006. Antibiotics modulate the stimulated cytokine response to endotoxin in a human ex vivo, in vitro model. *Acta Anaesthesiol Scand* 50:1103–1110. <https://doi.org/10.1111/j.1399-6576.2006.01112.x>.
54. Speer EM, Diago-Navarro E, Ozog LS, Dowling DJ, Hou W, Raheel M, Fries BC, Levy O. 2018. Pentoxifylline alone or in combination with gentamicin or vancomycin inhibits live microbe-induced proinflammatory cytokine production in human cord blood and cord blood monocytes. *Antimicrob Agents Chemother* 62:e01462-18. <https://doi.org/10.1128/AAC.01462-18>.
55. Rehli M. 2002. Of mice and men: species variations of Toll-like receptor expression. *Trends Immunol* 23:375–378. [https://doi.org/10.1016/s1471-4906\(02\)02259-7](https://doi.org/10.1016/s1471-4906(02)02259-7).
56. Tavakkol Z, Samuelson D, deLancey Pulcini E, Underwood RA, Usui ML, Costerton JW, James GA, Olerud JE, Fleckman P. 2010. Resident bacterial flora in the skin of C57BL/6 mice housed under SPF conditions. *J Am Assoc Lab Anim Sci* 49:588–591.
57. Mack D, Fischer W, Krokotsch A, Leopold K, Hartmann R, Egge H, Laufs R. 1996. The intercellular adhesin involved in biofilm accumulation of *Staphylococcus epidermidis* is a linear beta-1,6-linked glucosaminoglycan: purification and structural analysis. *J Bacteriol* 178:175–183. <https://doi.org/10.1128/jb.178.1.175-183.1996>.
58. Craig A, Luo NL, Beardsley DJ, Wingate-Pearse N, Walker DW, Hohimer AR, Back SA. 2003. Quantitative analysis of perinatal rodent oligodendrocyte lineage progression and its correlation with human. *Exp Neurol* 181:231–240. [https://doi.org/10.1016/S0014-4886\(03\)00032-3](https://doi.org/10.1016/S0014-4886(03)00032-3).
59. Albertsson AM, Bi D, Duan L, Zhang X, Leavenworth JW, Qiao L, Zhu C, Cardell S, Cantor H, Hagberg H, Mallard C, Wang X. 2014. The immune response after hypoxia-ischemia in a mouse model of preterm brain injury. *J Neuroinflammation* 11:153. <https://doi.org/10.1186/s12974-014-0153-z>.
60. Maderazo EG, Breaux S, Woronick CL, Krause PJ. 1990. Efficacy, toxicity, and pharmacokinetics of pentoxifylline and its analogs in experimental *Staphylococcus aureus* infections. *Antimicrob Agents Chemother* 34: 1100–1106. <https://doi.org/10.1128/aac.34.6.1100>.
61. Placencia FX, Kong L, Weisman LE. 2009. Treatment of methicillin-resistant *Staphylococcus aureus* in neonatal mice: lysostaphin versus vancomycin. *Pediatr Res* 65:420–424. <https://doi.org/10.1203/PDR.0b013e3181994a53>.
62. Sheldon RA, Sedik C, Ferriero DM. 1998. Strain-related brain injury in neonatal mice subjected to hypoxia-ischemia. *Brain Res* 810:114–122. [https://doi.org/10.1016/S0006-8993\(98\)00892-0](https://doi.org/10.1016/S0006-8993(98)00892-0).
63. Svedin P, Hagberg H, Mallard C. 2009. Expression of MMP-12 after neonatal hypoxic-ischemic brain injury in mice. *Dev Neurosci* 31: 427–436. <https://doi.org/10.1159/000232561>.
64. Ek CJ, D'Angelo B, Baburamani AA, Lehner C, Leverin A-L, Smith PLP, Nilsson H, Svedin P, Hagberg H, Mallard C. 2015. Brain barrier properties and cerebral blood flow in neonatal mice exposed to cerebral hypoxia-ischemia. *J Cereb Blood Flow Metab* 35:818–827. <https://doi.org/10.1038/jcbfm.2014.255>.